sustainability

MDPI

Article

Activated Biochar Is an Effective Technique for Arsenic Removal from Contaminated Drinking Water in Pakistan

Iftikhar Ahmad [1,*], Abdul Ghaffar [1], Ali Zakir [1], Zia Ul Haq Khan [1], Muhammad Farhan Saeed [1], Atta Rasool [1], Aftab Jamal [2,*], Adil Mihoub [3], Simone Marzeddu [4] and Maria Rosaria Boni [4]

[1] Department of Environmental Sciences, COMSATS University Islamabad, Vehari Campus, Vehari 61100, Pakistan
[2] Department of Soil and Environmental Sciences, Faculty of Crop Production Sciences, The University of Agriculture, Peshawar 25130, Pakistan
[3] Center for Scientific and Technical Research on Arid Regions, Biophysical Environment Station, Touggourt 30240, Algeria
[4] Department of Civil Construction and Environmental Engineering (DICEA), Faculty of Civil and Industrial Engineering, Sapienza University of Rome, Via Eudossiana 18, 00184 Rome, Italy
* Correspondence: iftikharahmad@cuivehari.edu.pk (I.A.); aftabses98@gmail.com (A.J.)

Abstract: Arsenic (As), the silent poison, is a widespread environmental pollutant which finds its way into drinking water supplies from natural or man-made sources and affects over 200 million people worldwide, including in Pakistan. It has been demonstrated that As causes serious health complications as well as social and economic losses. A quick, cost-effective, and simple method for efficiently filtering As from drinking water is urgently needed. The present study evaluates the ability of chemical treatment solutions to activate the sorption capacity of biochar derived from cotton stalks. The surface characteristics of CSB (cotton stalk biochar), HN-CSB (treated with nitric acid: HNO_3), and Na-CSB (treated with sodium hydroxide: NaOH) were investigated for their As sorption capacities and efficiency in removing As from contaminated drinking water. The chemical modification of biochar significantly increased the surface area and pore volume of CSB, with a maximum observed in HN-CSB (three times higher than CSB). Fourier-transform infrared spectroscopy (FTIR) analysis revealed several functional groups (OH^-, −COOH, C=O, N-H) on CSB, though the chemical modification of biochar creates new functional groups on its surface. Results showed that the maximum sorption capacity of CSB was (q = 90 μg g^{-1}), of Na-CSB was (q = 124 μg g^{-1}) and of HN-CSB was (q = 140 μg g^{-1}) at an initial As concentration of 200 μg L^{-1}, an adsorbent dose of 1 g L^{-1}, with 4 h of contact time, a pH of 6 and a temperature of 25 °C. However, As removal was found to be 45–88% for CSB, 62–94% for Na-CSB and 67–95% for HN-CSB across all As concentrations. An isotherm model showed that As sorption results were best fitted to the Langmuir isotherm model in the case of CSB (Q_{max} = 103 μg g^{-1}, R^2 = 0.993), Na-CSB (Q_{max} = 151 μg g^{-1}, R^2 = 0.991), and HN-CSB (Q_{max} = 157 μg g^{-1}, R^2 = 0.949). The development of the largest surface area, a porous structure, and new functional groups on the surface of HN-CSB proved to be an effective treatment for As removal from contaminated drinking water. Both HN-CSB and Na-CSB are clearly cost-effective adsorbents under laboratory conditions, but HN-CSB is cheaper and more efficient in As removal than Na-CSB, allowing it to be used as a powerful and promising adsorbent for the removal of pollutants like Arsenic from aqueous solution.

Keywords: arsenic; biochar; drinking water; human welfare; modification; remediation; Punjab (Vehari)

Citation: Ahmad, I.; Ghaffar, A.; Zakir, A.; Khan, Z.U.H.; Saeed, M.F.; Rasool, A.; Jamal, A.; Mihoub, A.; Marzeddu, S.; Boni, M.R. Activated Biochar Is an Effective Technique for Arsenic Removal from Contaminated Drinking Water in Pakistan. *Sustainability* **2022**, *14*, 14523. https://doi.org/10.3390/su142114523

Academic Editors: Shengsen Wang and Jun Wang

Received: 10 October 2022
Accepted: 1 November 2022
Published: 4 November 2022

1. Introduction

Heavy metal(loid)s are highly persistent are resistant to biological degradation, and accumulate in the fatty tissues, causing serious health problems [1–4]. Arsenic (As) is one of these highly toxic and carcinogenic metalloids [5,6]. Over the last decade, it has gained

considerable attention due to the high concentration of As in drinking water, which has been documented globally [6–9]. Recent reports have highlighted the emergence of arsenic poisoning in the residents of Argentina, Mexico, Chile, and Taiwan [3,10]. More than 105 countries worldwide have As contamination in ground water [2]. Ground water contamination with As has been reported in Taiwan, China, New Zeeland, India, Bangladesh, Canada, Poland, North Mexico, Hungry, Vietnam, Japan, the United States of America, Chile, Minnesota, Nepal, Spain, Pakistan, and Argentina [10–12]. Before the start of the 20th century, India, Bangladesh, China, and Pakistan were among the major regions of Asia with As contamination in ground water. More than 100 million people in these countries are at risk due to the use of water with As concentrations above the threshold limit [13]. Recently, studies and several news channels have drawn attention to the predicament of As contamination in groundwater above the threshold level in Pakistan [14,15], where residents using As-polluted water for drinking and domestic purposes are at a high risk of health problems. Microorganisms and different toxic compounds are the main factors behind surface and groundwater pollution in Pakistan [16]. Natural disasters, coupled with mismanagement and poor living conditions, often contaminate drinking water [17]. According to the latest survey and media reports, about 60 million people are at severe health risk in Pakistan due to use of As-contaminated water [14,15]. As a result, 20–40% of beds in Pakistani hospitals are occupied by patients suffering from waterborne diseases including cholera, diarrhea, dysentery, hepatitis, typhoid, etc. The poor quality of drinking water in Pakistan accounts for 40% of deaths and 50% of diseases [18,19]. Recently, water samples collected from the district Vehari showed that 95% of underground water is unfit for drinking [2,20].

Drinking water is a foremost source of As intake for humans [3,7]. Long-term As exposure causes several diseases and disorders, such as hyperkeratosis, circulatory disorders, bladder cancer, brain cancer, skin lesions and cancers, and cancer of the internal organs, even at very low concentration [8,9,21–23]. Studies have revealed that around 200 million people worldwide are exposed to different compounds of arsenic in drinking water at concentrations above the threshold limit of 10 $\mu g\ L^{-1}$ set by the WHO, the United States Environmental Protection Agency (USEPA), and the Food and Drug Administration (FDA) [3,5,14,23]. Considering the toxicity of As and the hazardous impact on human health, it is imperative to design techniques suitable for As treatment of drinking water. Arsenic exists in As^{-3}, As^{0}, As^{+3}, and As $^{+5}$ oxidation states [24], but approximately 90% of the total arsenic generally found in water is arenite (As^{+3}) and arsenate (As^{+5}) [7]. The efficiency of arsenic removal depends on the forms of arsenic present, as well as the nature of the water body, pH, temperature, contact time, concentration of metal ions, and the characteristics of the adsorbent [7,8,22,25].

Different techniques and methods have been used for the treatment of As in drinking and waste water, including coagulation-flocculation, oxidation, filtration, ion-exchange, membrane technologies, and adsorption [21]. Among the different conventional As removal techniques, the biosorption technique is efficient, eco-friendly, and cost effective [5,21,23,26]. Several adsorbent materials have been used in the past, such as activated carbon, synthetic resins alumina/silica oxide hydrate, red mud, dry plants, manganese oxide, laterite, fly ash, compost, granular ferric oxide, iron oxy-hydroxide, sand, zero-valent aluminum, zero-valent iron, etc. [2,21,27]

Over the last decade, researchers have tried to find low-cost and efficient naturally occurring adsorbents for the removal of arsenic from water [22]. Biochar has been extensively studied during the last decade as a soil amendment to improve soil fertility [28–31], but recently, it has been applied to water [32,33]. Biochar is a carbon-rich solid material produced through the burning of organic matter in a closed container with little or no air [31,34,35]. The physio-chemical properties of biochar, such as its three-dimensional reticulated and porous structure [36], might serve as a long-term carbon storage solution, while also adsorbing and decomposing contaminants [37]. Biochar may be made from a range of carbonaceous feedstocks, the majority of which are considered organic wastes;

hence, it indirectly supports waste management [38]. Biochar has been used in water and soil treatment as a low-cost material alternative to activated carbon for removing a variety of contaminants, such as volatile organic compounds, heavy metal ions, pesticides, pharmaceuticals, dyes, and polycyclic aromatic hydrocarbons, due to its cost-effective production and feasibility in a wide range of pollutants [39,40]. For low-cost and efficient treatment of As, biochar has gained substantial attention and has been studied extensively with regard to the treatment of As in soil and water [23,32,33]. Biochar is usually neutral to alkaline in nature, but acidic natures have also been reported. The feedstock type and production process (temperature, residence time) primarily have an effect on pH and the other properties of biochar, which have direct or indirect effects on the efficiency of metal(loid) removal [2].

In this study, cotton stalk was selected for biochar production because it is a low-cost adsorbent and is easily available. It contains cellulose, lignin, floristic fiber, and various functional groups that can adsorb heavy metal ions in aqueous solution [41]. Moreover, biochar prepared from cotton stalk has efficiently been applied to remove phosphate ion from water [42]. The researcher focused on the modification of the CSB surface and the production process to improve the efficiency of metal(loid) removal. Chemical modifications of biochar are frequently employed via reagents such as potassium hydroxide (KOH) [43,44], potassium permanganate ($KMnO_4$) [45], citric acid (CA) [46], and zinc chloride ($ZnCl_2$) [47]. Such biochar modifications offer more significant improvements to its physicochemical properties, such as specific surface area, pore size, molecular weight, cation exchange capacity (CEC), amount, and the type of functional groups [48,49].

Biochar adsorption has been a popular research field in recent years. Recently, it has been reported that chemical modification of CSB has increased the removal efficiency of metal ions (Pb^{+2}, Cd^{+2}, Ni^{+2}, PO_4^{3-}) from aqueous solution [42,43], but as far as we know, no studies have reported on the use of treated and untreated CSB to remove arsenate (AsV) and arsenite (AsIII) from drinking water, especially using the modification method or assessing the factors affecting the arsenic removal efficiency. The arsenate is a structural analog of phosphate ion; therefore, cotton stalk biochar (CSB) could be an efficient adsorbent material for As removal from water. As such, we hypothesized that the chemical modification of CSB surface using sodium hydroxide (NaOH) and nitric acid (HNO_3) might improve arsenic removal from drinking water. Thus, the aims of the present study are: (1) to characterize treated and untreated CSB using FTIR, SEM, and BET techniques, (2) to investigate the potential of treated and untreated CSB to be used for arsenic removal from contaminated drinking water, and (3) to explore the mechanisms behind arsenic removal using treated and untreated CSB. Moreover, the cost associated with the production of activated CSB was assessed to indicate its economic viability.

2. Materials and Method

A series of batch experiments were conducted in the Laboratory of COMSATS University Islamabad, Vehari Campus in order to evaluate the removal and adsorption efficiency of As using activated/non–activated cotton stalk biochar. An overview of the research methodology is presented in (Figure 1).

2.1. Preparation of Biochar

Cotton stalks (CS) were used for the preparation of biochar. Cotton stalks were collected from a field near COMSATS University Islamabad, Vehari Campus, Pakistan. The obtained cotton stalk biomass was cut into small pieces using a machine. To remove dust and other impurities, the cotton stalks were washed with de-ionized water several times, and for to remove moisture, they were oven dried at 60 °C for 24 h. The dried cotton stalk material was pyrolyzed at a low temperature (400 °C) in a muffle furnace under anaerobic conditions. In the pyrolysis process, the temperature rate was set at 7 °C/min until the target temperature was achieved. After reaching the target temperature, the sample was kept in a furnace for 1 h. Next, the biochar was grinded and sieved to obtain a uniform

particle size. The prepared biochar was removed and stored in airtight bags for further use.

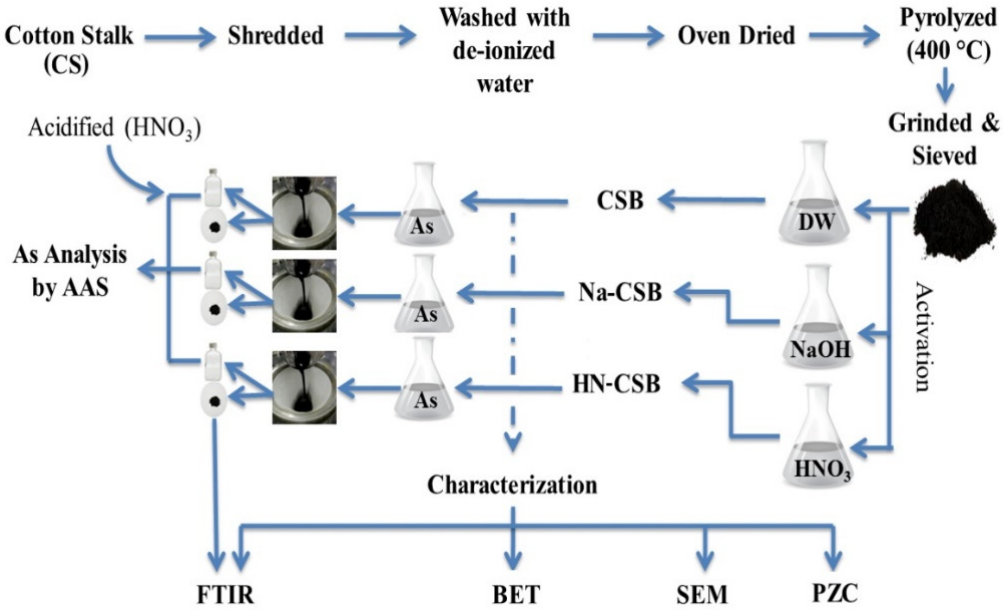

Figure 1. Flowchart presenting biochar preparation, activation, characterization, and application for As removal.

2.2. Chemical Activation of Biochar with Acid (HNO_3) and Base (NaOH)

The cotton stalk biochar (CSB) was soaked in either a 1 M HNO_3 and 1 M NaOH (analytical grade, Sigma-Aldrich, Darmstadt, Germany) solution at a mass to volume ratio of 1.0:25.0 in a 250 mL conical flask on a mechanical shaker set to 150 rpm for 4 h. The suspension was filtered with Whatman filter paper and dried at room temperature for 72 h. Additionally, to remove moisture content, the filtrate was oven dried at 100 °C for 1 h [43]. The CSB modified with HNO_3 and with NaOH were tagged as "HN-CSB" and "Na-CSB", respectively, and stored in airtight jars for further use.

2.3. Point of Zero Charge

Point of zero charge (PZC) was measured using the salt addition method [50,51]. In the present study, a 0.1 M NaCl background solution was prepared to make solutions of various pH (2, 4, 6, 8, and 10) adjusted with 0.1 M HCl or 0.1 M NaOH solutions. To avoid the dilution effect, the total volume of acid and base solution added was less than 5% of the sample volume. About 25 mL of NaCl solution for each pH maintained was agitated with 0.1 g of CSB, Na-CSB, or HN-CSB in a 250 mL conical flask, at room temperature, and on a mechanical shaker set to 150 rpm for 24 h. The suspension was then filtered with a Whatman filter and the final pH of the filtrate was measured. The differences between the final and initial pH values were then plotted against initial pH values, with the point of intersection being called pH_{pzc}.

2.4. Characterization of Activated and Non-Activated Biochar

To investigate the type of functional groups and surface characters of biochars (CSB, HN-CSB, and Na-CSB), FTIR, SEM, and BET techniques were used. Fourier-transform infrared spectroscopy (FTIR) spectra were conducted using an instrument made by Bruker, Germany (Model Vertex-70). Each sample was prepared for FTIR analysis by grinding and mixing 1 mg of the biochar with 200 mg of IR-grade KBr, and then each sample was pressed into a pellet using a hydraulic press. The FTIR spectrum of the pellet was recorded over a wavenumber range of 500 cm^{-1}–4500 cm^{-1}. SEM micrographs were obtained using a Jeol SEM (Model: JXA-840A, Tokyo, Japan) instrument. For this analysis, a solid sample homogeneously dispersed in pure ethanol was deposited on a Cu grid, previously covered

with a thin layer of biochar. The working potential difference was maintained at 15 or 20 kV in a vacuum depending on the sample. The total pore volume and specific surface area of the CSB, HN-CSB, and Na-CSB were measured using the Brunauer–Emmett–Teller (BET, Tristar II 3020).

2.5. Preparation of As-Contaminated Water

Four water samples were artificially contaminated with various levels of As (50, 100, 150, and 200 μg L^{-1}). For this purpose, a stock solution of 5000 μg L^{-1} As was prepared in the laboratory by dissolving sodium arsenite salt ($NaAsO_2$, analytical grade, Sigma-Aldrich) in distilled water.

2.6. Batch Biosorption Experiments

Batch biosorption experiments were conducted to explore the effects adsorbents (CSB, HN-CSB, Na-CSB) on As removal and sorption under variable biosorbent biomass and initial As concentrations in water. The sorption of As was determined by adding different doses (1.0, 2.0, and 3.0 g per L) of each biosorbent (CSB, HN-CSB, Na-CSB) to each As concentration (50, 100, 150, 200 μg L^{-1}). A solution's pH (6.0 ± 0.1) was maintained by adding 0.1 M HCl or 0.1 M NaOH solution. The suspension was shaken on a mechanical shaker at 150 rpm for 2 h at room temperature (25 ± 1 °C). The samples were then removed and filtered with Whatman filter paper. A few drops of 6 M HNO_3 were added to the samples, which were then stored at room temperature, prior to As analysis using Atomic Absorption Spectrophotometer (PinAAcle 900 series). As removal efficiency (%) and As sorption capacity (μg g^{-1}) of the three biochars were calculated as illustrated elsewhere [52].

$$\text{As Removal Efficiency } (\%) = \left(\frac{As_i - As_f}{As_i}\right) \times 100 \quad (1)$$

$$\text{As Sorption } (\mu g/g) = \left(\frac{As_i - As_f}{M_{CSB}}\right) \times V \quad (2)$$

where As_i (μg L^{-1}) and As_f (μg L^{-1}) are the initial and final concentrations of As in a supernatant, V (L) is the volume of the As-containing solution, and M_{CSB} (g) is the dry mass of the CSB adsorbent. The sorption capacity of As represented by Equation (2) was greatly influenced by adsorption type (multilayer, monolayer, chemical, or physical adsorption) [2].

2.7. Isotherm Modeling

Biochar offers the physical and electrostatic attachment of As to its surface [34]. At given temperature and pH, an isotherm is a curve to describe characteristics of adsorption at equilibrium [2]. There are several isotherm models available, but the most commonly used models for adsorption are the Langmuir and Freundlich isotherm adsorption models [2].

2.8. Langmuir Isotherm Model

The Langmuir model best represents the monolayer adsorption on the surface of an adsorbent [2,53]. All sides of a biochar have a uniform capability of holding adsorbate, and adsorption takes place on homogenous surface [53]. The Langmuir isotherm model is represented in Equation (3).

$$q = \frac{K_L q_{max} C_e}{1 + K_L C_e} \quad (3)$$

where K_L (L^3 M^{-1}) is a constant of the Langmuir model, q_{max} is the maximum sorption capacity of As (μg g^{-1}), and C_e is the concentration of As solution at equilibrium (μg g^{-1}). The linear form of the Langmuir model (Equation (3)) is represented by the following expression:

$$\frac{C_e}{q} = \frac{1}{q_{max} K_L} + \frac{1}{q_{max}} C_e \quad (4)$$

Langmuir parameters K_L and q_{max} were calculated from the intercept and slope of the linear plot of C_e versus $\frac{C_e}{q}$ by Equation (4)

2.9. Freundlich Isotherm Model

The Freundlich isotherm model best represents the relationship between reversible and non-ideal adsorption, not limited to monolayer formation. The Freundlich model can be very useful for multilayer adsorption, and when there is a non-uniform distribution of adsorption over the heterogeneous surface [2,53]. The Freundlich isotherm model is represented by following empirical relation:

$$q = K_F C_e^{1/n} \quad (5)$$

where q ($\mu g\ g^{-1}$) is the amount of adsorbed As at equilibrium, C_e is the concentration of As solution at equilibrium ($\mu g\ L^{-1}$), K_F is an indicator of adsorption capacity and called the Freundlich distribution coefficient, and n is an empirical parameter giving the adsorption intensity of the adsorbent material. A higher value of n indicates a higher proportion of adsorbate to adsorbent. The values of K_F and n were calculated from the intercept and slope by plotting the linear form of the Freundlich Equation (5). The plot was plotted against log q and log C_e according to the linear form of the Freundlich isotherm model, represented by the following equation:

$$\log q = \log K_F + \frac{1}{n} \log C_e \quad (6)$$

2.10. Data Analysis and Cost Estimation

Microsoft Excel pack 10 was used to calculate the As sorption and removal efficiency of three types of biochar (CSB, HN-CSB, Na-CSB). The Langmuir and Freundlich models were applied in Excel to calculate model parameters and to determine linear and non-linear relations. MS Excel was also used to create graphs. A cost analysis was performed to examine whether the production process of the activation char is feasible or not. The cost of producing 1 kg of chemically activated biochar in US dollars (USD) was determined. The cost analysis considers cost-influencing factors such as raw material availability, collection, treatment conditions, pyrolysis, and activation. Cost analysis was carried out by following the methods of Viotti et al. [54] and Chakraborty et al. [55].

3. Results

3.1. Point of Zero Charge of CSB, HN-CSB, and Na-CSB Results

The addition of CSB, HN-CSB, and Na-CSB to a solution of NaCl at different pH levels had altered the initial pH of the solution. To identify the Point of Zero Charge (PZC), the difference in pH was plotted against initial pH values, where the PZC is the point of intersection (Figure 2). In the case of acid-treated biochar, ΔpH increased sharply at pH values of 2–6 and thereafter decreased as compared to initial pH values. For Na-CSB, the values of ΔpH increased in pH range 2–8, but decreased sharply at pH 10. The ΔpH values of CSB sharply increased at pH values 2–6, but decreased at pH values 8–10. The increase in ΔpH values showed the alkaline nature of all three biochars. The curves for NaCl and HN-CSB intersect at ≈6.9 (Figure 2a), NaCl and Na-CSB intersect at ≈8.4 (Figure 2b), and NaCl and CSB intersect at ≈7.6 (Figure 2c), hence pH_{pzc} are neutral to alkaline, viz., 6.9, 7.6 and 8.4 for HN-CSB, CSB, and Na-CSB, respectively.

3.2. Chemical Characterization of Biosorbents

3.2.1. FTIR Analysis of CSB

The FTIR spectra of CSB before and after As loading showed a number of peaks which indicating the complex nature of biochar (Figure 3). To identify the different functional groups, the peak-by-peak correlation of untreated CSB before and after As loading were compared. Results revealed that CSB contains a number of different functional groups

which allow great potential for As sorption. The FTIR spectra have proved the changes in surface properties and functional groups of biochar before and after As treatment. An absence in and shifting of some functional groups' peaks have been observed after As loading. These changes were seen in the band present between 3500 and 3700 cm^{-1}, which may lead to hydroxyl (O-H) stretching free of H-bonds. Peaks shifted slightly in the bands ranging from 3000 to 3100 cm^{-1}, and 2840 to 2950 cm^{-1}, which were assigned to =C-H stretching alkene and –C-H stretching alkane compounds, and may have led to an ion-exchange process. Peaks were observed around 1821 cm^{-1}, which identified the carbonyl group (C=O) stretching in both spectra. Changes were seen around 1695 cm^{-1} which may be assigned to the aromatic (C=C) stretching group. The changes in peaks and absorbance difference observed between 1508 and 1498 cm^{-1} may be due to strong stretching nitro compounds (N-O). The peak observed at 1360 cm^{-1} is responsible for the nitro stretching group. The alcoholic (C-O) stretching functional group was found around 1150 cm^{-1}. The peaks observed around 950 and 890 cm^{-1} denoted the alkene (C=C) bending functional group. The new peak developed at 808 cm^{-1}, confirming the loading of As corresponding to C-H strong bending. The appearance and disappearance of peaks, shifting of peaks, reduction and enhancement of peaks, and changes in absorbance intensity might be due to As adsorption through different mechanisms, such as ion-exchange, precipitation, electrostatic attraction, and formation of complexes.

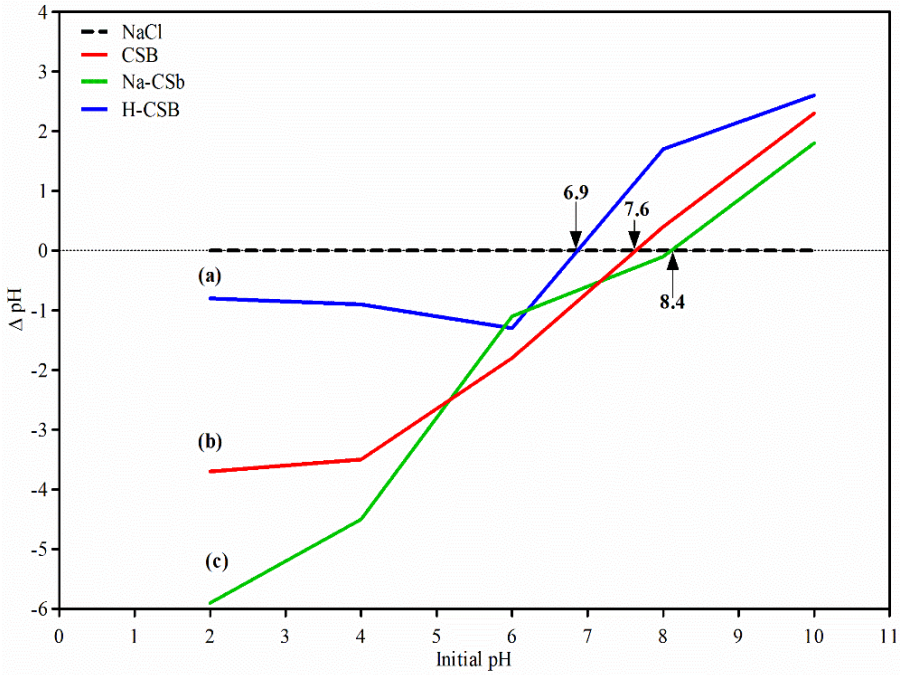

Figure 2. Point of zero charge for (**a**) H-NCSB, (**b**) CSB, and (**c**) Na-CSB. pH_{pzc} is the point where the ΔpH of the adsorbent intersects the ΔpH of NaCl.

3.2.2. FTIR Analysis of Na-CSB

FTIR analyses were carried out to determine the functional groups present in Na-CSB before and after As loading (Figure 4). A very broad peak observed from 3200 to 3500 cm^{-1} indicated alcohol O-H stretching intermolecular H-bonds. The spectra in this region shifted the peak after the As loading with high intensity. The multiple vibration bands observed around 2900 cm^{-1} may be associated with C-H stretching in the spectra of Na-CSB before As loading, but after As loading, these multiple bands converted into a single peak with a slight shift in wave number at high intensity. Major changes seen in band ranging from 2250 to 2380 cm^{-1} denoted a strong carbon dioxide (O=C=O) stretching group. A sharp peak observed at 2350 cm^{-1} in the carbon dioxide stretching group in the spectra of Na-CSB completely vanished after As loading. A small and intense peak occurred after As loading

at 1980 cm^{-1}, which is missing before As sorption and may be assigned to medium alkene (C=C=C) stretching compounds.

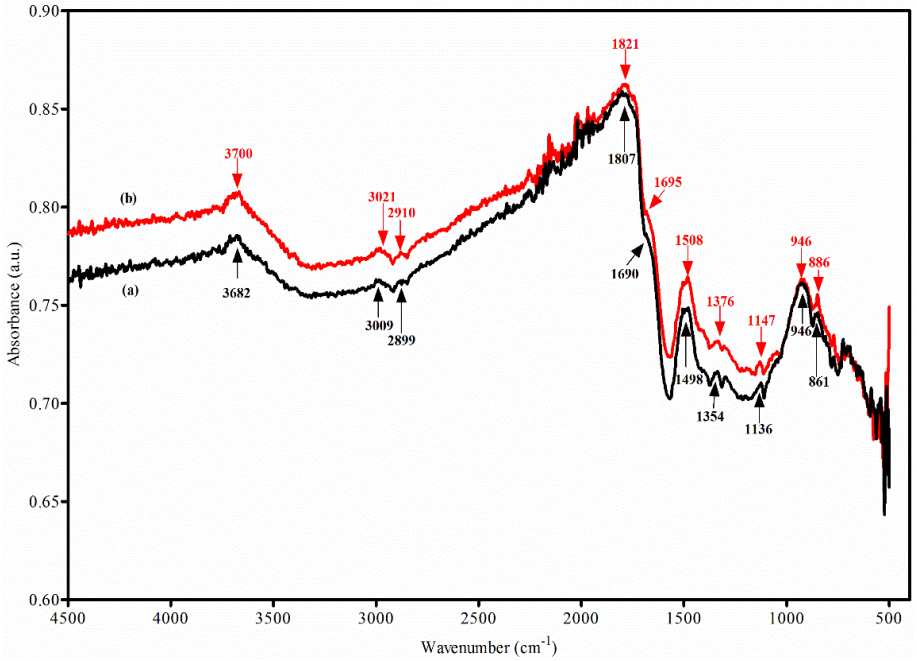

Figure 3. FTIR analysis of CSB (**a**) before and (**b**) after arsenic loading.

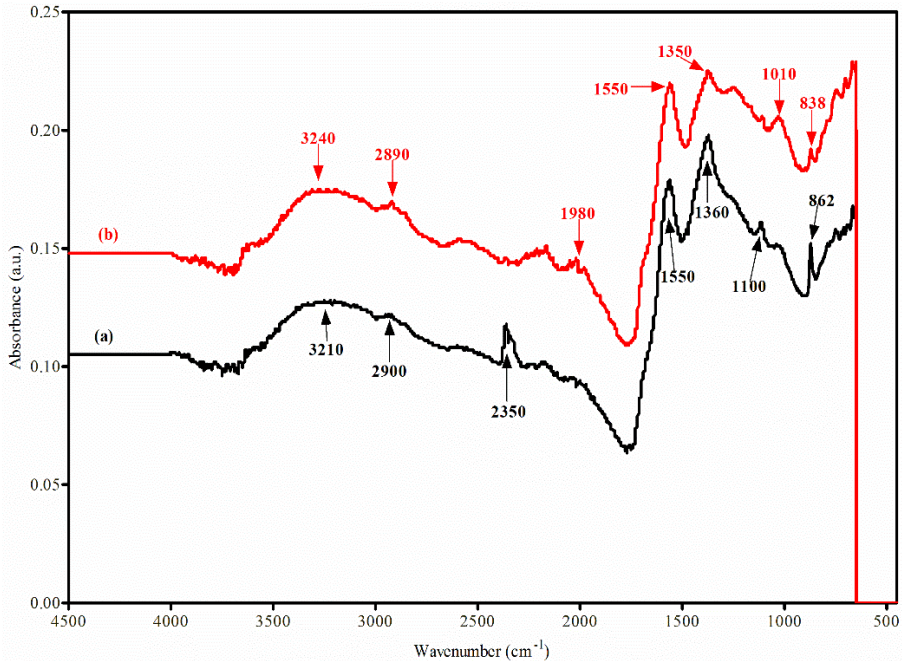

Figure 4. FTIR analysis of Na-CSB (**a**) before and (**b**) after As loading.

A peak occurred at 1550 cm^{-1} in both spectra, denoting strong N-O stretching nitro compounds. A large reduction in peaks after As loading around 1350 cm^{-1} occurred due to the attraction of As ions with strong (S=O) stretching sulfone compounds. A small but sharp peak of C-O stretching strong secondary alcohol was observed around 1100 cm^{-1}, which completely disappeared after As loading. The appearance and disappearance of peaks, shifting of peaks, reduction and enhancement of peaks, and changes in absorbance intensity might play significant role in As adsorption through different mechanisms such as ion-exchange, precipitation, electrostatic attraction, and formation of complexes.

3.2.3. FTIR Analysis of HN-CSB

To ensure the potential of acid-treated biochar (HN-CSB), FTIR spectra were analyzed before and after As loading (Figure 5). Major changes were observed in the form of reductions or enhancements in peaks, denoting functional groups, shifting in these peaks, and the appearance and disappearance of peaks after As loading. The production of multiple bands' peaks around 3500 to 3700 cm^{-1} is clearly an indication of newly formed strong hydroxyl (O-H) stretching free of the H-bonding functional group, which was negligible before the As loading, and might be due to complexation between hydroxyl and arsenic species. Peaks at 2900 cm^{-1} are responsible for the C-H stretching alkane group. A small peak appeared at 2150 cm^{-1} before As loading, which converted into a very broad peak around 2170 cm^{-1}; this might be due to the interaction of As species with stretching alkyne (-C≡C-) compounds.

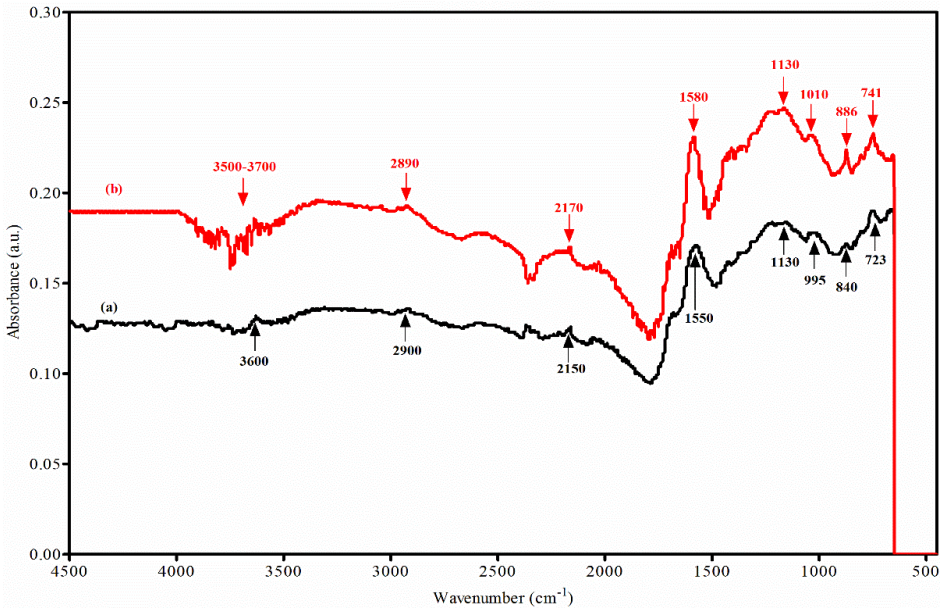

Figure 5. FTIR analysis of HN-CSB (**a**) before and (**b**) after As loading.

After the As loading of acid-treated biochar, a huge, sharp peak occurred around 1580 cm^{-1}, which has a different absorbance intensity as compared to the unloaded As spectrum. This change may be assigned to the chemical contact of As with strong N-O stretching nitro compounds. Peaks observed around 1130 cm^{-1} can be assigned to (O-H) alcohols (primary and secondary) and aliphatic ethers. Peaks observed around 1000 cm^{-1} are responsible for the (C-O) stretching of the COOH functional group. Peaks observed in FTIR spectra band 720 to 890 cm^{-1} may be assigned to (C-H) bending.

3.3. Morphological, Structural, and Textural Characteristics of Biochars

To estimate the biosorption mechanisms, microscopic analyses of the biosorbents' (CSB, Na-CSB, and HN-CSB) surfaces were conducted by scanning electron microscopy (SEM). Figure 6 shows the surface morphology of treated and un-treated biochars. Dissimilar surface morphology was observed for all treated and un-treated biochars. The surface morphologies of treated biochars were quite different to those of un-treated biochars; they were changed due to the addition of a base (1 M NaOH) or an acid (1 M HNO_3). The SEM photographs of CSB showed dense and firm particle structure with visible pores before As loading (Figure 6a), while HN-CSB (Figure 6c) and Na-CSB (Figure 6e) showed more crumbly, porous and distorted surfaces. The pores of untreated biochars were blocked with excess distribution of basic elements compounds; however, chemical modification with alkali and acid solutions removed substantial amounts of these basic compounds and exposed the surface of the biochar. Furthermore, base-treated biochar showed more

attractive surface for ion diffusion than other biochars. Poor pore distribution on the surface of untreated biochar was enhanced after chemical modification.

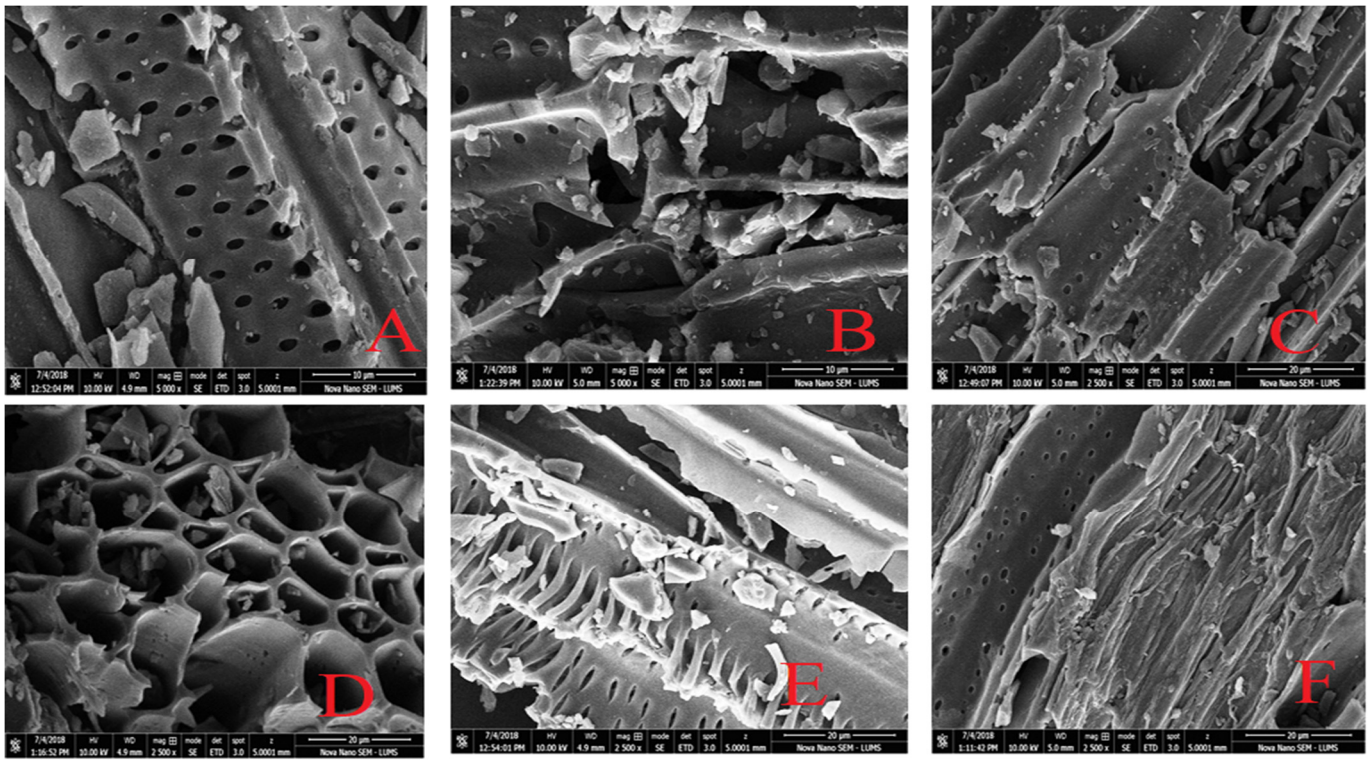

Figure 6. SEM photographs of biosorbents: (**A**) CSB, (**B**) CSB after As loaded, (**C**) HN-CSB, (**D**) HN-CSB after As loaded, (**E**) Na-CSB, and (**F**) Na-CSB after As loaded.

The surfaces of biosorbents after chemical modification were more amorphous and rough, with abundant protuberance, and numerous pores were available on the surface to facilitate the diffusion of As species ions on biosorbents. Surface modification after chemical treatment of biochar had considerable effects on surface area and pore volume of the activated biochar, and these results are consistent with BET determination of surface area and pore volume. After arsenic loading, the available pores on biosorbents (CSB, HN-CSB, and Na-CSB) were filled with arsenic species. The effects of acid and base treatment on the surface area and total pore volume of biochars was investigated using the BET method. Textural characterizations of treated and un-treated biochars are given in Table 1. The treatment introduced significant changes in the textural characterization of biochar. Alkaline- and acid-treated biochar showed an almost two- and three-fold increase in total pore volume over CSB, which enhanced the conditions for As adsorption. Acid-treated biochar show almost three-fold surface area and total pore volume as compared to CSB. Table 1 shows that acid and base treatment of CSB enhanced pore development and surface area during the activation process. According to the BET, the surface area of Na-CSB was increased by 26% and that of HN-CSB by 177% as compared to CSB. The chemical activation has a much higher impact on material porosity. It was found that both activated biochars had higher pore volumes compared with CSB, with the total pore volume of HN-CSB expanding from 0.155 $cm^3\ g^{-1}$ to 0.512 $cm^3\ g^{-1}$.

Table 1. Surface area and total pore volume of treated and un-treated biochars.

Biochar	Surface Area ($m^2\ g^{-1}$)	Total Pore Volume ($cm^3\ g^{-1}$)
CSB	103.62	0.155
Na-CSB	130.41	0.313
HN-CSB	287.82	0.512

3.4. Sorption of As

The results of this study revealed that acid- and base-modified CSB had higher removal and sorption capacities for As in contaminated water than untreated CSB. The effects of initial As concentration on As sorption and removal are shown in (Figure 7). The As removal efficiency decreased with an increase in initial As concentration, whereas the sorption capacity of As increased with an increase in initial As concentration, independent of the type of CSB used. As compared to CSB and Na-CSB, the HN-CSB led to a considerable increase in As removal efficiency. The maximum As removal efficiency was observed at 50 μg L^{-1} and the minimum at 200 μg L^{-1}, whereas the maximum sorption capacity of As was observed at 200 μg L^{-1} and the minimum was 50 μg L^{-1}. The maximum As removal efficiency by CSB, Na-CSB, and HN-CSB was found to be at the initial As concentration of 50 μg L^{-1} (88%, 2 g L^{-1}), and the minimum was detected at 200 μg L^{-1} (62%, 3 g L^{-1}); meanwhile, the sorption capacity of As was observed at its lowest at 50 μg L^{-1} (14.38 μg g^{-1}, 3 g L^{-1}) and at its highest at 200 μg L^{-1} (89.66 μg L^{-1}, 1 g L^{-1}). Na-CSB showed a maximum As removal efficiency at 50 μg L^{-1} (89%, 3 g L^{-1}) and a minimum was observed at 200 μg L^{-1}(62%, 1 g L^{-1}), whereas the minimum sorption capacity of As was noticed at initial concentration of 50 μg L^{-1} (14.89 μg g^{-1}, 3 g L^{-1}), and maximum sorption was observed at 200 μg L^{-1} (124.09 μg g^{-1}, 1 g L^{-1}). HN-CSB showed a maximum As removal efficiency at the initial concentration of 50 μg L^{-1} (95%, 1 g L^{-1}), and a minimum at 200 μg L^{-1} (67%, 3 g L^{-1}).

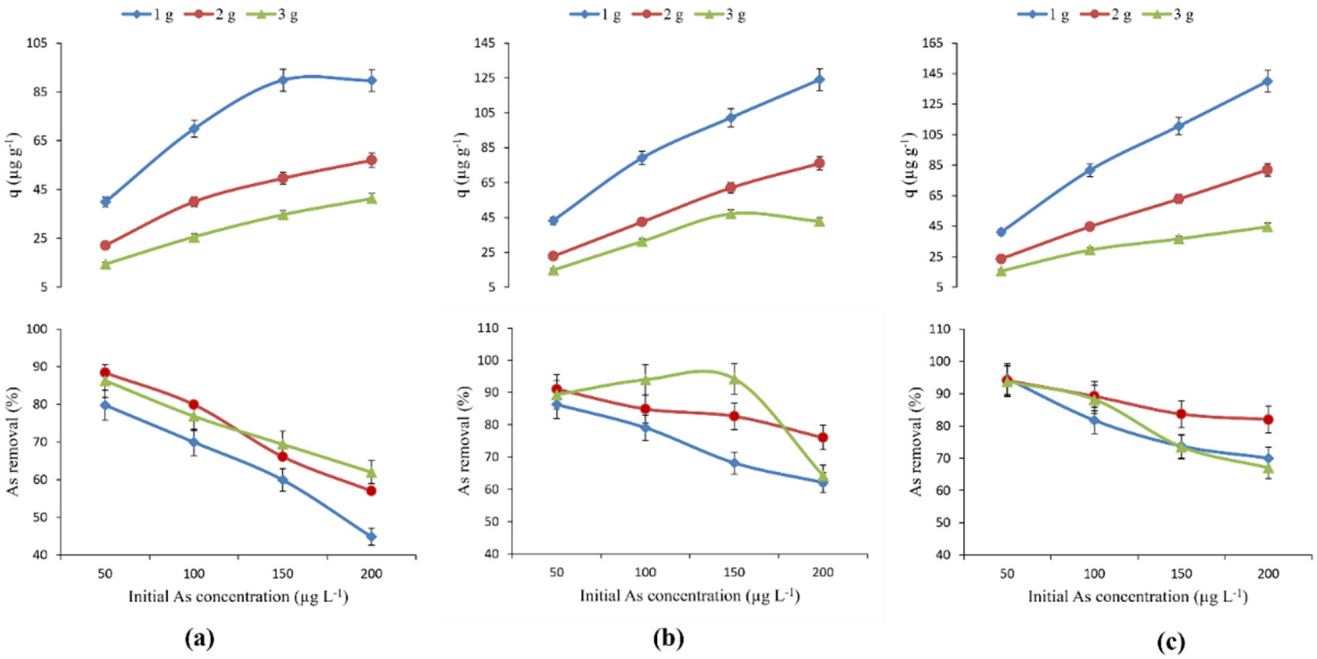

Figure 7. Effect of initial As concentration on As sorption and removal for (**a**) CSB, (**b**) Na-CSB, and (**c**) HN-CSB. Values are presented as standard error of means (n = 3).

The dose of adsorbent is a key factor that plays a significant role in the biosorption of As. The removal efficiency and sorption capacity of As were determined at different adsorbent doses (1.0, 2.0, and 3.0 g L^{-1}) as shown in (Figure 8). It can be seen that when biomass was increased from 1.0 to 3.0 g L^{-1} in As-contaminated water, the As removal efficiency increased from 45% to 88% (Figure 8), whereas the sorption capacity of As decreased from q = 88.28 to 44.83 μg g^{-1}. As removal increased when Na-CSB biomass was increased to 2.0 g L^{-1}, but a further increase in biomass to 3 g L^{-1} served to reduce As removal efficiency. The maximum sorption (q = 124.09 μg g^{-1}) was observed at 1.0 g L^{-1}, whereas the minimum sorption (q = 14.89 μg g^{-1}) occurred at 3.0 g L^{-1}. Acid-treated biochar showed the same trend as base-treated biochar: As removal efficiency increased

up to 2.0 g L^{-1} and then decreased after a further increase in the biomass of HN-CSB (Figure 8). It was observed that when the biomass of HN-CSB biosorbent increased from 1.0 to 2.0 g L^{-1}, the As removal efficiency = increased (70% to 95%), but then decreased (95% to 67%) due to further increase in the biomass of HN-CSB. The sorption of As reached its maximum (q = 140 µg g^{-1}) and minimum (q = 15.62 µg g^{-1}) at a biomass of 1.0 and 2.0 g L^{-1}, respectively.

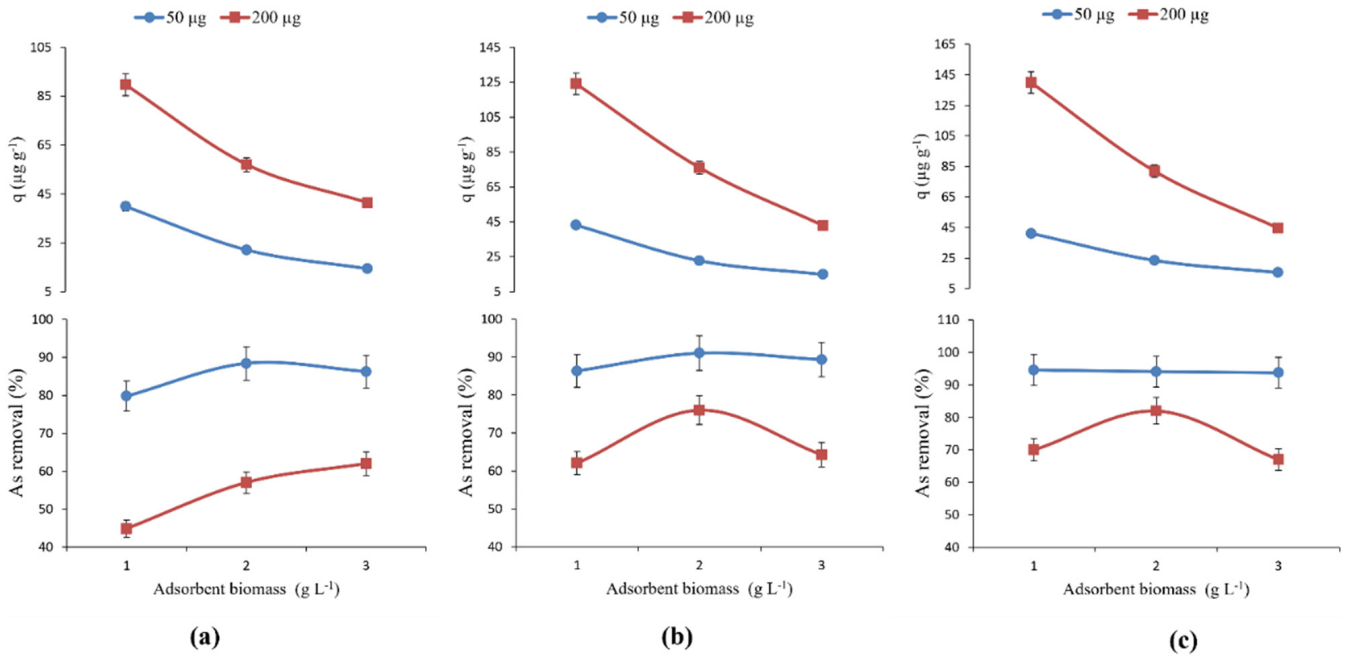

Figure 8. Effect of adsorbent dose on As sorption and removal (**a**) CSB, (**b**) Na-CSB, and (**c**) HN-CSB. Values are presented as standard error of means (n = 3).

3.5. Adsorption Isotherm

The biosorption of As by CSB, Na-CSB, and HN-CSB was analyzed using the Freundlich and Langmuir isotherms models at various adsorbent doses. The linear form of the Langmuir isotherm was plotted between C_e versus Ce/q, and between ln q versus ln C_e for the Freundlich isotherm. The slope and intercept used to determine other parameters and data of the isotherms are presented in Table 2. To determine the best fit isotherm model for the sorption of As, the R^2 values of both models were compared. It was observed that the Langmuir and Freundlich models simulated the experimental isotherms well with good R^2 values. The isotherms' data showed that the Langmuir isotherm model was best fitted for the sorption of As by CSB (R^2 = 0.993) and Na-CSB (R^2 = 0.991), whereas it was least suited to HN-CSB (R^2 = 0.949). In most cases, the Langmuir model had a greater value of R^2 than the Freundlich model for isotherm, except for HN-CSB, where the Freundlich isotherm model was better fitted than the Langmuir isotherm model, based on their R^2 values. This showed that heterogeneous surface properties formed after acid treatment. Large values of the K_f coefficient indicated larger adsorption capacity, whereas the value of coefficient n indicates the strength of the adsorbent material used. Low values of n showed weak bonds between the adsorbent and adsorbate materials. The values of n and K_f obtained for HN-CSB were 2.952 and 32.733, respectively. HN-CSB showed a maximum sorption of As in contaminated water (Q_{max} = 156.94 µg g^{-1}) which slightly higher than Na-CSB (Q_{max} = 151.01 µg g^{-1}), and the least sorption was observed in untreated CSB (Q_{max} = 102.78 µg g^{-1}).

Table 2. Langmuir and Freundlich adsorption isotherm parameters for As biosorption on cotton stalk biochar (CSB), sodium hydroxide-treated (Na-CSB), and nitric acid-treated (HN-CSB) biochar.

Biochar	Langmuir Isotherm			Freundlich Isotherm		
	Qmax (μg g^{-1})	K_L (L μg^{-1})	R^2	n	K_F (μg g^{-1})	R^2
CSB	102.78	0.07	0.993	2.206	15.169	0.981
Na-CSB	151.01	0.05	0.991	2.316	19.601	0.985
HN-CSB	156.94	0.09	0.949	2.952	32.733	0.983

Qmax: maximum sorption capacity, KL: constant of Langmuir model, n: empirical parameter giving adsorption intensity of adsorbent material, KF: indicator of adsorption capacity.

3.6. Cost Analysis

It is important for researchers to analyze the cost effectiveness of adsorbent materials for the targeted community in order to assess the utilization of biochar derived from cotton stock (CSB) that is normally considered as an agricultural residue in cotton growing areas of Pakistan. In addition, the overall cost of producing the adsorbent for commercial use influences the farming community, as it provides an alternative to high-cost products available in the market. In general, adsorbent cost estimation involves different steps, like raw material collection, size reduction, pyrolysis and steam activation, calcification, etc. Other factors such as the availability of raw material, treatment conditions, process requirements and reusability are also important to consider during cost analysis, as adsorbent selection and application depend on these and the above-mentioned factors. The costs of producing 1 kg of CSB, HN-CSB, and Na-CSB in US dollars (USD) have been listed in Table 3. The cost analysis of CSB, HN-CSB, and Na-CSB suggests that the adsorbent preparation process from cotton stalk is cost effective. The total costs incurred to derive 1 kg of R-CSB, HN-CSB, and Na-CSB biochar from cotton stalk at laboratory-scale have been calculated as PKR 255.00, PKR 767.60, and PKR 902.07, respectively. It has clearly been observed from the calculations that the production cost incurred by the steam activation of CSB is comparatively cheaper as compared to the cost of HN-CSB and Na-CSB, due to the utilization of chemical reagents during their preparation. Despite having economic differences at small scales, chemical activation is effectively required to improve the favorable characteristics of an adsorbent, like the surface area, uptake capacity, and micro-pore volume. The cost estimations of chemically activated adsorbents evidently concluded that both HN-CSB and Na-CSB are cost effective adsorbents under laboratory conditions; however, HN-CSB, owing to it being the cheaper option and more efficient in removal compared to Na-CSB, can be used as an effective and promising adsorbent for the removal of contaminants from aqueous solution.

Table 3. Cost estimation of biochar prepared from cotton stalk (CSB) and treated with nitric acid (HN-CSB) or sodium hydroxide (Na-CSB).

Type of Biochar	Operational Parameters	Break Up Cost	Total Cost (USD)
		Cotton stalk biochar (CSB)	
Cost of CSB	Raw material collection cost	Collected from local farmers free of cost	0
	Cleaning cost	material was cleaned using distilled water: hours × units × per unit cost (1 × 0.5 × 0.047)	0.0235
	Size reduction cost	hours × units × per unit cost (0.25 × 1 × 0.047)	0.0117
	Drying cost	hours × units × per unit cost (12 × 1 × 0.047)	0.564
	Pyrolysis cost	hours × units × unit cost (2 × 3 × 0.047)	0.282
	Steam activation cost	superheated steam production cost + heating cost = (hours × units × per unit cost) + (hours × units × per unit cost) = (1 × 0.8 × 0.047) + (1 × 1.5 × 0.047)	0.1081
Net cost			0.9893
	Overhead (10%)		0.0989
Total cost			1.088

Table 3. *Cont.*

Type of Biochar	Operational Parameters	Break Up Cost	Total Cost (USD)
		HNO_3 activated cotton stalk biochar (HN-CSB)	
		Cost of CSB	1.088
	Cost of HN-CSB	Heating cost = hours × units × per unit cost (1 × 1.5 × 0.047)	0.0705
		Cost of HNO3	1.81
		Total cost	2.968
	Overhead (10%)		0.2968
Total cost			3.265
		NaOH activated cotton stalk biochar (Na-CSB)	
Cost of CSB			1.088
	Cost of Na-CSB	Heating cost = hours × units × per unit cost (1 × 1.5 × 0.047)	0.0705
		Cost of NaOH	2.33
		Total cost	3.488
	Overhead (10%)		0.3488
Total cost			3.837

4. Discussion

4.1. PZC Analysis

Figure 2 demonstrated the pH behavior of all three biochars. The positive increase in the pH values of CSB, HN-CSB, and Na-CSB biochars in the range of pH 2–6 clearly identifies the neutral-to-alkaline nature of biochar [56]. Results showed that all three biochars used in the experiments had negative surface charge at a pH greater than 6.9, 8.4, and 7.6 for HN-CSB, Na-CSB, and CSB, respectively. Figure 2 shows the surface charge of the biosorbents at different pH values. The negative charge of the biochars at a high pH had a significant impact on adsorbing As. If the pH of the solution is greater than $pH_{PZC,}$ then the solution will have more OH^- ions, whereas when the solution has a pH lower than $pH_{PZC,}$ it generates more H^+ ions in the solution. The arsenic species present in the contaminated water were mostly in the form of anions, so for better removal results, the pH of the solution should be lower than the pH_{PZC}. We selected a pH of 6.0 ± 0.1 for all biosorption studies in this work, because choosing a lower pH value than the pH_{PZC} of CSB, Na-CSB, and HN-CSB generated more H+ ions, which are appropriate for strong interactions with anionic As species [57].

4.2. FTIR Analysis of Biosorbents

The FTIR spectra of CSB, HN-CSB, and Na-CSB were analyzed before and after As loading. Different peaks in the FTIR spectra before and after As loading denoted different functional groups, and these groups might have the potential for As sorption from contaminated water [43]. It can be seen clearly that the FTIR spectra showed variations in absorption before and after As loading (Figures 3–5). The disappearance and appearance of some peaks, the shifting of peaks, reduction and enchantment in peaks sharpness, and changes in the intensity of transmittance are evidence of interaction of As species with the different functional groups present in the biosorbents [1,43,58].

4.2.1. FTIR Analysis of CSB

After As loading, the peak of the hydroxyl (O-H) stretching group at 3700 cm^{-1} changed and high absorbance was observed, confirming the formation of complexes of As species, with different compounds of OH stretching through hydrogen bonding [58]. Peaks present at 3009, 2899, 1821, 1690, 1498, 1354, and 1136 cm^{-1} in CSB before As loading shifted after As loading (Figure 3), which might be assigned to As sorption through ion-exchange, precipitation, electrostatic attraction, or complexes. After As loading, the increase in the intensity of absorbance may be assigned to the presence of less functional groups after As loading [59].

4.2.2. FTIR Analysis of Na-CSB

Before and after As loading, the Na-CSB FTIR spectra were analyzed to reveal the possible methods of As sorption (Figure 4). After As loading, the peak of OH stretching hydroxyl group, previously present at 3210 cm^{-1}, shifted to 3240 cm^{-1}, which may suggest that alcoholic OH compounds were also responsible for As sorption through H-boning [1]. A peak originally at 2900 cm^{-1} shifted after the loading of As. A sharp peak occurred at 2350 cm^{-1} in virgin Na-CSB spectra, denoting strong carbon dioxide (O=C=O) stretching group, which completely disappeared after As loading. A new sharp peak appeared at 838 cm^{-1} after As loading, and showed the sorption of As in the form of As-O [60].

4.2.3. FTIR Analysis of HN-CSB

Major changes occurred in the absorbance ranging from 3500 to 3700 cm^{-1}, which may be assigned to hydroxyl (O-H) stretching compounds. A small peak at 3600 cm^{-1} was converted into multiple band peaks with different intensities [61]. Peaks appeared at 2900, 2150, and 995, which had slightly shifted after As loading. The peaks of stretching alkyne (-C≡C-) and stretching nitro (N-O) compounds at 2170, 1580, and 1510 cm^{-1} showed more sharper peaks after As loading than in the virgin biochar. These imply that the compounds of alkynes (-C≡C-) stretching, ketone, and nitro are involved in As sorption [60].

4.3. Morphological, Structural, and Textural Characteristics of Biochars

In order to estimate the biosorption mechanisms, microscopic analysis of the biosorbents' (CSB, Na-CSB, and HN-CSB) surfaces were determined by SEM before and after As loading. Chemical modification of biochar with acid and base significantly increased the BET surface area and pore volume compared to untreated biochar (Table 2). Previous study has revealed that alkali treatment of biochar could cleanup blocked pores of biochar, which enhanced its porosity [62]. The main mechanism involved in surface area and pore volume changes is a reaction between the alkali and basic compounds present in biochar [63]. In the present study, the surface area of alkali-treated biochar increased from 103.62 m^2/g to 130.41 m^2/g, and pore volume from 0.155 cm^3/g to 0.313 cm^3/g after NaOH treatment of biochar. This might be due to the formation of meso-pores and macro-pores through the destruction of the nano-pores' structure [64]. It has been reported that the acidic modification of biochar could produce major changes in the physicochemical properties of an adsorbent [65]. Pine tree biochar treated with H_3PO_4 showed higher surface area than virgin biochar. It was also reported that as H_3PO_4 percentage was increased, the surface area and pore volume of activated biochar increased further [1]. In the present study, the surface area and total pore volume of acid-treated biochar were increased from 103.62 m^2/g to 287.82 m^2/g and 0.155 cm^3/g to 0.512 cm^3/g, respectively. The increases in surface area and in pore volume might facilitate the diffusion of As species ions into the biochar pores, and in this way, changes to the texture and structural properties offer more active sites to bind the metals ions to the surface of the biochar [66]. After As loading, the available pores on all biosorbents were filled (showed in SEM photograph); this might be due to the physical adsorption of arsenic species on the surface of biosorbents.

4.4. Sorption of As

The As removal efficiency and sorption capacities of chemically modified CSB were higher than un-treated CSB. Mosa et al. [43] conducted a study in which chemically treated and un-treated biochar were used to remove different metal ions. The study's results revealed that chemically modified biochar enhanced the removal and sorption of metal ions. The chemical modification of biochar increased the As uptake of Na-CSB and HN-CSB by 94% and 95%, respectively (Figures 7 and 8). Our results are consistent with these previous results; for instance, the removal efficiency of As ions increased with respect to an increase in adsorbent dose [67], whereas the As removal efficiency decreased after an increase in the initial concentration of As in the solution [43,68]. The increase in initial As concentrations led to an increase in sorption capacity of As by all three biochars, and similar

results have been reported by [23] that as the initial concentration of As (III) is increased from 0.05 to 7 mg L^{-1}, the sorption capacity increases from 0.01 to 2.91 mg g^{-1}. An increase in concentration of sorbent material, resulting strong built-up of concentration gradient among different As species oxyanions and biochar surface, led to significant increase in As sorption for all biochars [52]. It was observed that the sorption capacity of As ions decreased as biochar mass increased. This might be due to a partial increase in the mutual attraction between particles, which normally occurs at a higher biomass.

The increase in the removal efficiency of As ions with an increase in biochar biomass may be due to more surface area being available to adsorb more As ions [2]. Cottonseed hulls and soyabean modified with NaOH had improved sorption for Zn (II) as compared to un-modified variations [69]. NaOH-treated waste products had enhanced sorption capacity over un-treated materials [70]. The acid and base treatment of raw rice husk enhanced the sorption capacity of cadmium [71]. KOH activation of municipal solid waste biochar enhanced the adsorption capacity of arsenate ions from aqueous solution [64]. Our results confirmed all above findings suggesting that activated biochar shows promising effects on As removal and sorption over simple biochar. Although, we have found greater As removal efficiency (95%) and sorption capacity (q = 140 μg g^{-1}) by HN-CSB compared to Na-CSB and CSB. This might be due to high surface area and the diverse functional groups of HN-CSB. Moreover, SEM analysis revealed As loading on the surface of HN-CSB (Figure 6d) much more clearly than Na-CSB (Figure 6f) and CSB (Figure 6b).

4.5. Adsorption Isotherms

It was observed that the Langmuir and Freundlich models simulated the experimental isotherms well, with good R^2 values. The Langmuir isotherm model was best fitted for sorption of As with the highest R^2 values (R^2 = 0.993 for CSB, R^2 = 0.991 for Na-CSB), whereas the Freundlich isotherm model gave better results for HN-CSB (R^2 = 0.983, Table 2). In most cases, the Langmuir model had greater R^2 values than the Freundlich model for isotherm, with the exception of HN-CSB. Isotherm data revealed that un-treated CSB and base-treated CSB have monolayer adsorption for As ions. Similar results were reported in a study conducted by [64], which used municipal solid waste treated with 2 M KOH for As removal. The results revealed that the Langmuir isotherm model was the best fit for sorption data (R^2 > 0.95) for CSB and Na-CSB, which was contradictory to studies on biochar derived from cotton stalk (Zhang et al. 2018) and biochar derived from rice husk [72], which suggested that the Freundlich isotherm model gave better fit to adsorption data. But in case of HN-CSB, the Freundlich isotherm model gave better results than the Langmuir, which was supported by above mentioned studies. It has been reported that the Langmuir isotherm model gave better results than the Freundlich isotherm model for the sorption of cadmium ions using treated (with acid and base) and untreated rice husk biochar [71].

Biochar derived from perilla leaf was used to remove arsenite and arsenate ions from aqueous solution, and the results of sorption isotherms showed that the Langmuir isotherm model provided the best fit (R^2 = 0.97) [23]. Since both the Freundlich and Langmuir isotherm models explain, the As sorption isotherm follow the monolayer adsorption for Na-CSB and CSB, whereas the sorption of As by HN-CSB is not restricted to the monolayer adsorption process. A similar phenomenon was also observed in another relevant study conducted by [73]. The results of that study revealed that both the Langmuir and Freundlich isotherm models adequately explained the sorption data for raw and alkali-treated biochar, with the exception of acid-treated biochar. HN-CSB showed a maximum sorption of As from aqueous (Q_{max} = 156.94 μg g^{-1}) which was slightly higher than that of Na-CSB (Q_{max} = 151.01 μg g^{-1}), and was significant higher than untreated biochar (Q_{max} = 102.78 μg g^{-1}). Table 4 compares the sorption capacities of the current study with other research on arsenic removal from water using modified biochar over the past decade. Chemically modification biochar derived from cotton stalk with acid and base proved better adsorbent material than a number of adsorbent materials used for As removal.

Table 4. The sorption capacities of the current study with other research on arsenic removal from water using modified biochar over the past decade.

Adsorbent	Activation Media	Initial As conc. (μg L^{-1})	Max. Sorption (μg g^{-1})	Reference
Pine wood	Birnessite	10,000	910	[74]
Pine wood	Mn Oxide	10,000	590	[74]
Pinecone		100	6	[74]
Rice Husk		900	2.59	[72]
Activated Aluma		2000	560	[75]
Sand	Iron coated	2000	40	[75]
Rice Polish		1000	140	[76]
A. niger biomass	iron oxide coated	100	47	[77]
Fish Scale		1000	26	[78]
Bone Char		1500	22	[79]
Cotton Stalk Biochar		200	103	Present Study
Cotton Stalk Biochar	NaOH	200	151	Present Study
Cotton Stalk Biochar	HNO_3	200	157	Present Study

5. Conclusions

In this study, cotton stalks were selected for biochar production because they are a low-cost adsorbent, readily available, easy to operate, and compact unit processes, owing to which the technology is universally acceptable and commercially available. The study deals with an efficient approach to utilizing alkali- and acid-activated biochar and mitigating one of the most severe drinking water problems caused by arsenic. We hypothesized that acid and base treatment could improve the adsorption capacities of cotton stalk biochar. The results of this study have confirmed this hypothesis, and we showed high surface area, diverse functional groups, and porous structure of cotton stalk biochar, confirmed by the Brunauer-Emmett-Teller, Fourie—Transform Infrared Spectroscopy, and Scanning Electron Microscope, respectively. Base- and acid-treated biochar showed a maximum As removal of up to 94 and 95%, respectively, regardless of initial As concentration and adsorbent biomass. The Langmuir isotherm model showed a better fit to the adsorption data than the Freundlich model. The interaction of As with the biochar surface involved electrostatic attraction at pH < pH_{PZC}, ion exchange, physical adsorption, surface/co-precipitation, and surface complexes. Sorption isotherm study revealed that the chemical treatment of cotton stalk biochar with acid and base considerably increased As sorption capacities from 103 μg g^{-1} to 157 μg g^{-1} and 151 μg g^{-1}, respectively. The present study gives new insights into the ability of Na-CSB and HN-CSB biochar for As remediation in contaminated drinking water. Such information may also be used to provide practical ideas for future research into new types of biochar-based materials with super-strong As adsorption capability.

Author Contributions: Conceptualization, I.A.; methodology, I.A., A.G., A.J. and M.F.S.; software, I.A., and A.Z.; validation, A.G., Z.U.H.K., A.Z., A.R. and M.F.S.; formal analysis, M.F.S., Z.U.H.K. and I.A.; investigation, I.A., M.F.S. and A.G.; resources, M.F.S. and A.R.; data curation, I.A., A.Z. and M.F.S.; writing-original draft preparation, I.A., A.G. and M.F.S.; writing-review and editing, A.M., A.J., M.F.S., S.M. and M.R.B.; visualization, A.G. and Z.U.H.K.; supervision, M.F.S., A.G. and I.A.; project administration, I.A.; funding acquisition, S.M., M.R.B., A.J. and I.A. All authors have read and agreed to the published version of the manuscript.

Funding: The financial support from the Higher Education Commission of Pakistan under SRGP-project (Grant#21-293/SRGP/R&D/HEC/2014).

Data Availability Statement: Not applicable.

Acknowledgments: Authors gratefully acknowledge technical and financial support from the Sapienza University of Rome, Via Eudossiana, Rome, Italy.

Conflicts of Interest: The authors declare no conflict of interest.

References

1. Chen, D.; Awut, T.; Liu, B.; Ma, Y.; Wang, T.; Nurulla, I. Functionalized magnetic Fe_3O_4 nanoparticles for removal of heavy metal ions from aqueous solutions. *e-Polymers* **2016**, *16*, 313–322. [CrossRef]
2. Ahmad, I.; Akhtar, M.J.; Jadoon, I.B.K.; Imran, M.; Ali, S. Equilibrium modeling of cadmium biosorption from aqueous solution by compost. *Environ. Sci. Pollut. Res.* **2016**, *24*, 5277–5284. [CrossRef] [PubMed]
3. Shahid, M.; Khalid, M.; Dumat, C.; Khalid, S.; Niazi, N.K.; Imran, M.; Bibi, I.; Ahmad, I.; Hammad, H.M.; Tabassum, R.A. Arsenic Level and Risk Assessment of Groundwater in Vehari, Punjab Province, Pakistan. *Expo. Health* **2017**, *10*, 229–239. [CrossRef]
4. Jamal, A.; Sarim, M.J.W.S.N. Heavy metals distribution in different soil series of district Swabi, Khyber Pakhunkhawa, Pakistan. *World Sci. News* **2018**, *105*, 1–13.
5. Meher, A.K.; Das, S.; Rayalu, S.; Bansiwal, A. Enhanced arsenic removal from drinking water by iron-enriched aluminosilicate adsorbent prepared from fly ash. *Desalination Water Treat.* **2016**, *57*, 20944–20956. [CrossRef]
6. Ociński, D.; Jacukowicz-Sobala, I.; Mazur, P.; Raczyk, J.; Kociołek-Balawejder, E. Water treatment residuals containing iron and manganese oxides for arsenic removal from water—Characterization of physicochemical properties and adsorption studies. *Chem. Eng. J.* **2016**, *294*, 210–221. [CrossRef]
7. Asif, Z.; Chen, Z. Removal of arsenic from drinking water using rice husk. *Appl. Water Sci.* **2015**, *7*, 1449–1458. [CrossRef]
8. Hering, J.G.; Katsoyiannis, I.A.; Theoduloz, G.A.; Berg, M.; Hug, S.J. Arsenic Removal from Drinking Water: Experiences with Technologies and Constraints in Practice. *J. Environ. Eng.* **2017**, *143*, 03117002. [CrossRef]
9. Tuček, J.; Prucek, R.; Kolařík, J.; Zoppellaro, G.; Petr, M.; Filip, J.; Sharma, V.K.; Zbořil, R. Zero-Valent Iron Nanoparticles Reduce Arsenites and Arsenates to As(0) Firmly Embedded in Core–Shell Superstructure: Challenging Strategy of Arsenic Treatment under Anoxic Conditions. *ACS Sustain. Chem. Eng.* **2017**, *5*, 3027–3038. [CrossRef]
10. Rasool, A.; Farooqi, A.; Masood, S.; Hussain, K. Arsenic in groundwater and its health risk assessment in drinking water of Mailsi, Punjab, Pakistan. *Hum. Ecol. Risk Assess. Int. J.* **2015**, *22*, 187–202. [CrossRef]
11. Mondal, P.; Bhowmick, S.; Chatterjee, D.; Figoli, A.; Van der Bruggen, B. Remediation of inorganic arsenic in groundwater for safe water supply: A critical assessment of technological solutions. *Chemosphere* **2013**, *92*, 157–170. [CrossRef] [PubMed]
12. Shakoor, M.B.; Niazi, N.K.; Bibi, I.; Murtaza, G.; Kunhikrishnan, A.; Seshadri, B.; Shahid, M.; Ali, S.; Bolan, N.S.; Ok, Y.S.; et al. Remediation of arsenic-contaminated water using agricultural wastes as biosorbents. *Crit. Rev. Environ. Sci. Technol.* **2015**, *46*, 467–499. [CrossRef]
13. Chakraborti, D.; Das, B.; Rahman, M.M.; Nayak, B.; Pal, A.; Sengupta, M.K.; Ahamed, S.; Hossain, A.; Chowdhury, U.K.; Biswas, B.K.; et al. Arsenic in groundwater of the Kolkata Municipal Corporation (KMC), India: Critical review and modes of mitigation. *Chemosphere* **2017**, *180*, 437–447. [CrossRef] [PubMed]
14. Podgorski, J.E.; Eqani SA MA, S.; Khanam, T.; Ullah, R.; Shen, H.; Berg, M. Extensive arsenic contamination in high-pH unconfined aquifers in the Indus Valley. *Sci. Adv.* **2017**, *3*, e1700935. [CrossRef]
15. Sanjrani, M.A.; Mek, T.; Sanjrani, N.D.; Leghari, S.J.; Moryani, H.T.; Shabnam, A. Current situation of aqueous arsenic contamination in Pakistan, focused on Sindh and Punjab Province, Pakistan: A review. *J. Pollut. Eff. Cont.* **2017**, *5*, 2.
16. Azizullah, A.; Khattak, M.N.K.; Richter, P.; Häder, D.-P. Water pollution in Pakistan and its impact on public health—A review. *Environ. Int.* **2011**, *37*, 479–497. [CrossRef]
17. Rasheed, F.; Khan, A.; Kazmi, S.U. Bacteriological analysis, antimicrobial susceptibility and detection of 16S rRNA gene of Helicobacter pylori by PCR in drinking water samples of earthquake affected areas and other parts of Pakistan. *Malays. J. Microbiol.* **2009**, *5*, 123–127. [CrossRef]
18. Farooq, S.; Hashmi, I.; Qazi, I.A.; Qaiser, S.; Rasheed, S. Monitoring of Coliforms and chlorine residual in water distribution network of Rawalpindi, Pakistan. *Environ. Monit. Assess.* **2007**, *140*, 339–347. [CrossRef]
19. Daud, M.K.; Nafees, M.; Ali, S.; Rizwan, M.; Bajwa, R.A.; Shakoor, M.B.; Arshad, M.U.; Chatha, S.A.S.; Deeba, F.; Murad, W.; et al. Drinking Water Quality Status and Contamination in Pakistan. *BioMed Res. Int.* **2017**, *2017*. [CrossRef]
20. Ali, S.S.; Anwar, Z.; Khattak, J.Z.K. Microbial analysis of drinking water and water distribution system in new urban Peshawar. *Curr. Res. J. Biol. Sci.* **2012**, *4*, 731–737.
21. Nicomel, N.R.; Leus, K.; Folens, K.; Van Der Voort, P.; Du Laing, G. Technologies for Arsenic Removal from Water: Current Status and Future Perspectives. *Int. J. Environ. Res. Public Health* **2015**, *13*, 62. [CrossRef] [PubMed]
22. Kanel, S.R.; Choi, H. Removal of arsenic from groundwater by industrial byproducts and its comparison with zero-valent iron. *J. Hazard. Toxic Radioact. Waste* **2017**, *21*, 04016028. [CrossRef]
23. Niazi, N.K.; Bibi, I.; Shahid, M.; Ok, Y.S.; Burton, E.D.; Wang, H.; Shaheen, S.M.; Rinklebe, J.; Lüttge, A. Arsenic removal by perilla leaf biochar in aqueous solutions and groundwater: An integrated spectroscopic and microscopic examination. *Environ. Pollut.* **2018**, *232*, 31–41. [CrossRef] [PubMed]
24. Malik, A.H.; Khan, Z.M.; Mahmood, Q.; Nasreen, S.; Bhatti, Z.A. Perspectives of low cost arsenic remediation of drinking water in Pakistan and other countries. *J. Hazard. Mater.* **2009**, *168*, 1–12. [CrossRef] [PubMed]
25. Zhang, W.; Cho, Y.; Vithanage, M.; Shaheen, S.M.; Rinklebe, J.; Alessi, D.S.; Hou, C.-H.; Hashimoto, Y.; Withana, P.A.; Ok, Y.S. Arsenic removal from water and soils using pristine and modified biochars. *Biochar* **2022**, *4*, 1–26. [CrossRef]
26. Samad, A.; Fukumoto, T.; Dabwan, A.H.A.; Katsumata, H.; Suzuki, T.; Furukawa, M.; Kaneco, S. Enhanced Removal of Arsenite from Ground Water by Adsorption onto Heat-Treated Rice Husk. *Open J. Inorg. Non-Metallic Mater.* **2016**, *6*, 18–23. [CrossRef]

27. Mohamed CH IB, A.N.; Mohamed ZE RB, E.T.; Gabriela CA RJ, A.; Fouad SI NA, N. Application of low-cost adsorbents for arsenic removal: A review. *J. Environ. Chem. Ecotoxicol.* **2012**, *4*, 91–102. [CrossRef]
28. Turan, V. Confident performance of chitosan and pistachio shell biochar on reducing Ni bioavailability in soil and plant plus improved the soil enzymatic activities, antioxidant defense system and nutritional quality of lettuce. *Ecotoxicol. Environ. Saf.* **2019**, *183*, 109594. [CrossRef]
29. Turan, V. Potential of pistachio shell biochar and dicalcium phosphate combination to reduce Pb speciation in spinach, improved soil enzymatic activities, plant nutritional quality, and antioxidant defense system. *Chemosphere* **2019**, *245*, 125611. [CrossRef]
30. Turan, V. Arbuscular mycorrhizal fungi and pistachio husk biochar combination reduces Ni distribution in mungbean plant and improves plant antioxidants and soil enzymes. *Physiol. Plant.* **2021**, *173*, 418–429. [CrossRef]
31. Turan, V. Calcite in combination with olive pulp biochar reduces Ni mobility in soil and its distribution in chili plant. *Int. J. Phytoremediation* **2021**, *24*, 166–176. [CrossRef] [PubMed]
32. Park, J.H.; Choppala, G.K.; Bolan, N.S.; Chung, J.W.; Chuasavathi, T. Biochar reduces the bioavailability and phytotoxicity of heavy metals. *Plant Soil* **2011**, *348*, 439–451. [CrossRef]
33. Beesley, L.; Inneh, O.S.; Norton, G.J.; Moreno-Jimenez, E.; Pardo, T.; Clemente, R.; Dawson, J.J. Assessing the influence of compost and biochar amendments on the mobility and toxicity of metals and arsenic in a naturally contaminated mine soil. *Environ. Pollut.* **2014**, *186*, 195–202. [CrossRef] [PubMed]
34. Ahmad, M.; Rajapaksha, A.U.; Lim, J.E.; Zhang, M.; Bolan, N.; Mohan, D.; Vithanage, M.; Lee, S.S.; Ok, Y.S. Biochar as a sorbent for contaminant management in soil and water: A review. *Chemosphere* **2014**, *99*, 19–33. [CrossRef]
35. Mohan, D.; Sarswat, A.; Ok, Y.S.; Pittman, C.U., Jr. Organic and inorganic contaminants removal from water with biochar, a renewable, low cost and sustainable adsorbent—A critical review. *Bioresour. Technol.* **2014**, *160*, 191–202. [CrossRef]
36. Marzeddu, S.; Décima, M.A.; Camilli, L.; Bracciale, M.P.; Genova, V.; Paglia, L.; Marra, F.; Damizia, M.; Stoller, M.; Chiavola, A.; et al. Physical-Chemical Characterization of Different Carbon-Based Sorbents for Environmental Applications. *Materials* **2022**, *15*, 7162. [CrossRef]
37. Tauqeer, H.M.; Basharat, Z.; Ramzani, P.M.A.; Farhad, M.; Lewińska, K.; Turan, V.; Karczewska, A.; Khan, S.A.; Faran, G.-E.; Iqbal, M. Aspergillus niger-mediated release of phosphates from fish bone char reduces Pb phytoavailability in Pb-acid batteries polluted soil, and accumulation in fenugreek. *Environ. Pollut.* **2022**, *313*, 120064. [CrossRef]
38. Amin, A.E.E.A.Z.; Mihoub, A. Effect of sulfur-enriched biochar in combination with sulfur-oxidizing bacterium (*Thiobacillus* spp.) on release and distribution of phosphorus in high calcareous p-fixing soils. *J. Soil Sci. Plant Nutr.* **2021**, *21*, 2041–2047. [CrossRef]
39. El-Naggar, A.; Ahmed, N.; Mosa, A.; Niazi, N.K.; Yousaf, B.; Sharma, A.; Sarkar, B.; Cai, Y.; Chang, S.X. Nickel in soil and water: Sources, biogeochemistry, and remediation using biochar. *J. Hazard. Mater.* **2021**, *419*, 126421. [CrossRef]
40. Rasool, B.; Rahman, M.U.; Zubair, M.; Khan, M.A.; Ramzani, P.M.A.; Dradrach, A.; Turan, V.; Iqbal, M.; Khan, S.A.; Tauqeer, H.M.; et al. Synergetic Efficacy of Amending Pb-Polluted Soil with P-Loaded Jujube (Ziziphus mauritiana) Twigs Biochar and Foliar Chitosan Application for Reducing Pb Distribution in Moringa Leaf Extract and Improving Its Anti-cancer Potential. *Water Air Soil Pollut.* **2022**, *233*, 1–21. [CrossRef]
41. Nada, A.M.A.; El-Wakil, N.A.; Hassan, M.L.; Adel, A.M. Differential adsorption of heavy metal ions by cotton stalk cation-exchangers containing multiple functional groups. *J. Appl. Polym. Sci.* **2006**, *101*, 4124–4132. [CrossRef]
42. Ren, J.; Li, N.; Li, L.; An, J.-K.; Zhao, L.; Ren, N.-Q. Granulation and ferric oxides loading enable biochar derived from cotton stalk to remove phosphate from water. *Bioresour. Technol.* **2015**, *178*, 119–125. [CrossRef] [PubMed]
43. Mosa, A.A.; El-Ghamry, A.; Al-Zahrani, H.; Selim, E.M.; El-Khateeb, A. Chemically modified biochar derived from cotton stalks: Characterization and assessing its potential for heavy metals removal from wastewater. *Environ. Biodivers. Soil Secur.* **2017**, *1*, 33–45.
44. Tan, G.; Sun, W.; Xu, Y.; Wang, H.; Xu, N. Sorption of mercury (II) and atrazine by biochar, modified biochars and biochar based activated carbon in aqueous solution. *Bioresour. Technol.* **2016**, *211*, 727–735. [CrossRef]
45. Wang, H.; Gao, B.; Wang, S.; Fang, J.; Xue, Y.; Yang, K. Removal of Pb (II), Cu (II), and Cd (II) from aqueous solutions by biochar derived from KMnO4 treated hickory wood. *Bioresour. Technol.* **2015**, *197*, 356–362. [CrossRef]
46. Mihoub, A.; Amin, A.E.-E.A.Z.; Motaghian, H.R.; Saeed, M.F.; Naeem, A. Citric Acid (CA)–Modified Biochar Improved Available Phosphorus Concentration and Its Half-Life in a P-Fertilized Calcareous Sandy Soil. *J. Soil Sci. Plant Nutr.* **2021**, *22*, 465–474. [CrossRef]
47. Shen, B.; Li, G.; Wang, F.; Wang, Y.; He, C.; Zhang, M.; Singh, S. Elemental mercury removal by the modified bio-char from medicinal residues. *Chem. Eng. J.* **2015**, *272*, 28–37. [CrossRef]
48. Nazari, S.; Rahimi, G.; Nezhad, A.K.J. Effectiveness of native and citric acid-enriched biochar of Chickpea straw in Cd and Pb sorption in an acidic soil. *J. Environ. Chem. Eng.* **2019**, *7*, 103064. [CrossRef]
49. Takaya, C.; Fletcher, L.; Singh, S.; Anyikude, K.; Ross, A. Phosphate and ammonium sorption capacity of biochar and hydrochar from different wastes. *Chemosphere* **2016**, *145*, 518–527. [CrossRef]
50. Mahmood, T.; Saddique, M.T.; Naeem, A.; Westerhoff, P.; Mustafa, S.; Alum, A. Comparison of Different Methods for the Point of Zero Charge Determination of NiO. *Ind. Eng. Chem. Res.* **2011**, *50*, 10017–10023. [CrossRef]
51. Liu, Z.; Xue, Y.; Gao, F.; Cheng, X.; Yang, K. Removal of ammonium from aqueous solutions using alkali-modified biochars. *Chem. Speciat. Bioavailab.* **2016**, *28*, 26–32. [CrossRef]
52. Abid, M.; Niazi, N.K.; Bibi, I.; Farooqi, A.; Ok, Y.S.; Kunhikrishnan, A.; Ali, F.; Ali, S.; Igalavithana, A.D.; Arshad, M. Arsenic (V) biosorption by charred orange peel in aqueous environments. *Int. J. Phytoremediation* **2016**, *18*, 442–449. [CrossRef] [PubMed]

53. Kazak, O.; Eker, Y.R.; Akin, I.; Bingol, H.; Tor, A. Green preparation of a novel red mud@ carbon composite and its application for adsorption of 2, 4-dichlorophenoxyacetic acid from aqueous solution. *Environ. Sci. Pollut. Res.* **2017**, *24*, 23057–23068. [CrossRef] [PubMed]
54. Viotti, P.; Tatti, F.; Rossi, A.; Luciano, A.; Marzeddu, S.; Mancini, G.; Boni, M.R. An Eco-Balanced and Integrated Approach for a More-Sustainable MSW Management. *Waste Biomass-Valorization* **2020**, *11*, 5139–5150. [CrossRef]
55. Chakraborty, P.; Show, S.; Banerjee, S.; Halder, G. Mechanistic insight into sorptive elimination of ibuprofen employing bi-directional activated biochar from sugarcane bagasse: Performance evaluation and cost estimation. *J. Environ. Chem. Eng.* **2018**, *6*, 5287–5300. [CrossRef]
56. Yoon, K.; Cho, D.-W.; Tsang, D.C.; Bolan, N.; Rinklebe, J.; Song, H. Fabrication of engineered biochar from paper mill sludge and its application into removal of arsenic and cadmium in acidic water. *Bioresour. Technol.* **2017**, *246*, 69–75. [CrossRef]
57. El Zayat, M.; Smith, E. Modeling of heavy metals removal from aqueous solution using activated carbon produced from cotton stalk. *Water Sci. Technol.* **2013**, *67*, 1612–1619. [CrossRef]
58. Zhang, F.; Wang, X.; Xionghui, J.; Ma, L. Efficient arsenate removal by magnetite-modified water hyacinth biochar. *Environ. Pollut.* **2016**, *216*, 575–583. [CrossRef]
59. Boddu, V.M.; Abburi, K.; Talbott, J.L.; Smith, E.D.; Haasch, R. Removal of arsenic (III) and arsenic (V) from aqueous medium using chitosan-coated biosorbent. *Water Res.* **2008**, *42*, 633–642. [CrossRef]
60. Zheng, Y.-M.; Lim, S.F.; Chen, J.P. Preparation and characterization of zirconium-based magnetic sorbent for arsenate removal. *J. Colloid Interface Sci.* **2009**, *338*, 22–29. [CrossRef]
61. Lin, L.; Qiu, W.; Wang, D.; Huang, Q.; Song, Z.; Chau, H.W. Arsenic removal in aqueous solution by a novel Fe-Mn modified biochar composite: Characterization and mechanism. *Ecotoxicol. Environ. Saf.* **2017**, *144*, 514–521. [CrossRef] [PubMed]
62. Regmi, P.; Moscoso, J.L.G.; Kumar, S.; Cao, X.; Mao, J.; Schafran, G. Removal of copper and cadmium from aqueous solution using switchgrass biochar produced via hydrothermal carbonization process. *J. Environ. Manag.* **2012**, *109*, 61–69. [CrossRef] [PubMed]
63. Trakal, L.; Šigut, R.; Šillerová, H.; Faturíková, D.; Komárek, M. Copper removal from aqueous solution using biochar: Effect of chemical activation. *Arab. J. Chem.* **2014**, *7*, 43–52. [CrossRef]
64. Jin, H.; Capareda, S.; Chang, Z.; Gao, J.; Xu, Y.; Zhang, J. Biochar pyrolytically produced from municipal solid wastes for aqueous As(V) removal: Adsorption property and its improvement with KOH activation. *Bioresour. Technol.* **2014**, *169*, 622–629. [CrossRef]
65. Bakshi, S.; Banik, C.; Rathke, S.J.; Laird, D.A. Arsenic sorption on zero-valent iron-biochar complexes. *Water Res.* **2018**, *137*, 153–163. [CrossRef]
66. Vithanage, M.; Herath, I.; Joseph, S.; Bundschuh, J.; Bolan, N.; Ok, Y.S.; Kirkham, M.; Rinklebe, J. Interaction of arsenic with biochar in soil and water: A critical review. *Carbon* **2017**, *113*, 219–230. [CrossRef]
67. Fan, J.; Xu, X.; Ni, Q.; Lin, Q.; Fang, J.; Chen, Q.; Shen, X.; Lou, L. Enhanced As (V) Removal from Aqueous Solution by Biochar Prepared from Iron-Impregnated Corn Straw. *J. Chem.* **2018**, *2018*, 1–8. [CrossRef]
68. Zhu, N.; Zhang, J.; Tang, J.; Zhu, Y.; Wu, Y. Arsenic removal by periphytic biofilm and its application combined with biochar. *Bioresour. Technol.* **2018**, *248*, 49–55. [CrossRef]
69. Hu, X.; Ding, Z.; Zimmerman, A.R.; Wang, S.; Gao, B. Batch and column sorption of arsenic onto iron-impregnated biochar synthesized through hydrolysis. *Water Res.* **2015**, *68*, 206–216. [CrossRef]
70. Kumar, A.; Namdeo, M.; Mehta, R.; Agrawala, V. Effect of arsenic contamination in potable water and its removal techniques. *Int. J. Water Wastewater Treat* **2015**, *1*, 1–11.
71. Kumar, U.; Bandyopadhyay, M. Sorption of cadmium from aqueous solution using pretreated rice husk. *Bioresour. Technol.* **2006**, *97*, 104–109. [CrossRef] [PubMed]
72. Agrafioti, E.; Kalderis, D.; Diamadopoulos, E. Arsenic and chromium removal from water using biochars derived from rice husk, organic solid wastes and sewage sludge. *J. Environ. Manag.* **2014**, *133*, 309–314. [CrossRef] [PubMed]
73. Liu, P.; Liu, W.-J.; Jiang, H.; Chen, J.-J.; Li, W.-W.; Yu, H.-Q. Modification of bio-char derived from fast pyrolysis of biomass and its application in removal of tetracycline from aqueous solution. *Bioresour. Technol.* **2012**, *121*, 235–240. [CrossRef] [PubMed]
74. Wang, S.; Gao, B.; Zimmerman, A.R.; Li, Y.; Ma, L.; Harris, W.G.; Migliaccio, K.W. Removal of arsenic by magnetic biochar prepared from pinewood and natural hematite. *Bioresour. Technol.* **2015**, *175*, 391–395. [CrossRef] [PubMed]
75. Sinha, R.; Kumar, R.; Abhishek, K.; Shang, J.; Bhattacharya, S.; Sengupta, S.; Kumar, N.; Singh, R.K.; Mallick, J.; Kar, M.; et al. Single-step synthesis of activated magnetic biochar derived from rice husk for hexavalent chromium adsorption: Equilibrium mechanism, kinetics, and thermodynamics analysis. *Groundw. Sustain. Dev.* **2022**, *18*. [CrossRef]
76. Ranjan, D.; Talat, M.; Hasan, S.H. Biosorption of arsenic from aqueous solution using agricultural residue 'rice polish'. *J. Hazard. Mater.* **2009**, *166*, 1050–1059. [CrossRef]
77. Pokhrel, D.; Viraraghavan, T. Arsenic Removal from Aqueous Solution by Iron Oxide-Coated Biomass: Common Ion Effects and Thermodynamic Analysis. *Sep. Sci. Technol.* **2008**, *43*, 3545–3562. [CrossRef]
78. Rahaman, M.; Basu, A.; Islam, M. The removal of As(III) and As(V) from aqueous solutions by waste materials. *Bioresour. Technol.* **2008**, *99*, 2815–2823. [CrossRef]
79. Chen, Y.-N.; Chai, L.-Y.; Shu, Y.-D. Study of arsenic(V) adsorption on bone char from aqueous solution. *J. Hazard. Mater.* **2008**, *160*, 168–172. [CrossRef]